FOC Neutral Density Filter Throughputs

W. Hack and M. Voit
March 18, 1997

ABSTRACT

We analyze a series of observations taken with different neutral density filter combinations yielding new measurements of the neutral density filter throughputs. This report describes the observation set, the method of photometry, and how potential problems with the data were avoided. These new measurements provide a different result from previous internal calibrations, and various reasons for this discrepancy are discussed at the end of this report. In general, the 1ND, 2ND and 4ND filters appear to be within 3% of the expected throughputs for the F430W bandpass. However, there may be a significant color effect which will be investigated with further calibration observations.

1. Introduction

The FOC's photon-counting nature requires bright targets to be imaged through neutral density filters in order to safeguard the instrument and to obtain photometrically correct observations. The FOC Instrument Handbook clearly states that stars brighter than B=9 or diffuse sources with a surface brightness greater than 10 magnitudes arcsec^{-2} in the F430W filter would exceed the safety limits. These limits correspond to count rates of 10^6 photons s^{-1} pix^{-1} at the peak of a point source and 100 photons s^{-1} pix^{-1} over the entire photocathode for a diffuse source. Targets approaching these limits may be observed only through filters that bring the observed count rates down into the linear regime. The f/96 camera of the FOC possesses 5 neutral density filters for this purpose: F1ND on filter wheel 3 and F2ND, F4ND, F6ND, and F8ND on filter wheel 1. The numerals correspond roughly to the number of magnitudes of attenuation each filter provides, and the F1ND filter can be used in tandem with each of the others. Usually observers using the 512x512 format of the f/96 camera will want to reduce the observed signal to less than 1 counts s^{-1} pix^{-1} in the peak of a point source or 0.15 counts s^{-1} pix^{-1} across a diffuse source. At higher count rates, the response of the FOC detectors becomes >10% non-linear and even-

tually saturates. Consult section 6.2 of the FOC Instrument Handbook for more details and recommended count rates for other detector formats.

Recent and upcoming FOC observations of some of the brightest stars in the sky have underscored the need for neutral density filters and the importance of calibrating them properly. These observations were planned using the expected throughputs of the filters as given in the Calibration Database System (CDBS). Most of these filter transmission curves are based on ground-based measurements taken prior to launch, and the throughputs of the netural density filters have undergone only a modest amount of in-orbit verification. This report describes a set of observations of a crowded stellar field taken through the F430W filter with many different ND filter combinations. The next section decribes this set of observations, and Section 3 discusses the data analysis, including the method of photometry and a description of the results. Section 4 compares these new results with previous calibrations of the ND filters, and Section 5 describes strategies for new calibrations to confirm our present understanding of these results.

Table 1. Summary of Observations from Proposal 5518 Used for Analysis

Rootname	Filters	Exp. Time	Format
x2bw0109t	F430W F6ND F1ND	1795.875	512x512
x2bw010at	F430W F6ND	1495.875	“
x2bw010bt	F430W F4ND F1ND	1039.875	“
x2bw010ct	F430W F4ND	995.875	“
x2bw010dt	F430W F2ND F1ND	995.875	“
x2bw010ft	F430W F2ND	508.875	“
x2bw010gt	F430W F1ND	595.875	“

2. Calibration Observations

Filter calibrations benefit from many separate measurements that can be used to reduce the statistical errors. The core of NGC5139 (ω Cen) provides many stars of widely varying magnitudes, even in the small FOC field of view. Proposal 5518 was designed to image this field through the F430W filter and a range of ND filters from F1ND to F6ND+F1ND. This scheme produced multiple images of the same set of stars throughout a large range of ND filter transparencies. The only differences between the images were the amounts of ND filters used and the exposure times, as shown in Table 1. Since the stars varied widely in magnitude, there were usually a number of stars with linear count rates in each image. Figure 1 shows two of the images from the dataset, each taken with a different set of NDs to illustrate the sample of stars available for photometry.

Figure 1: (**a**)F430W+F1ND image and (**b**) F430W+F6ND+F1ND image of NGC5139.

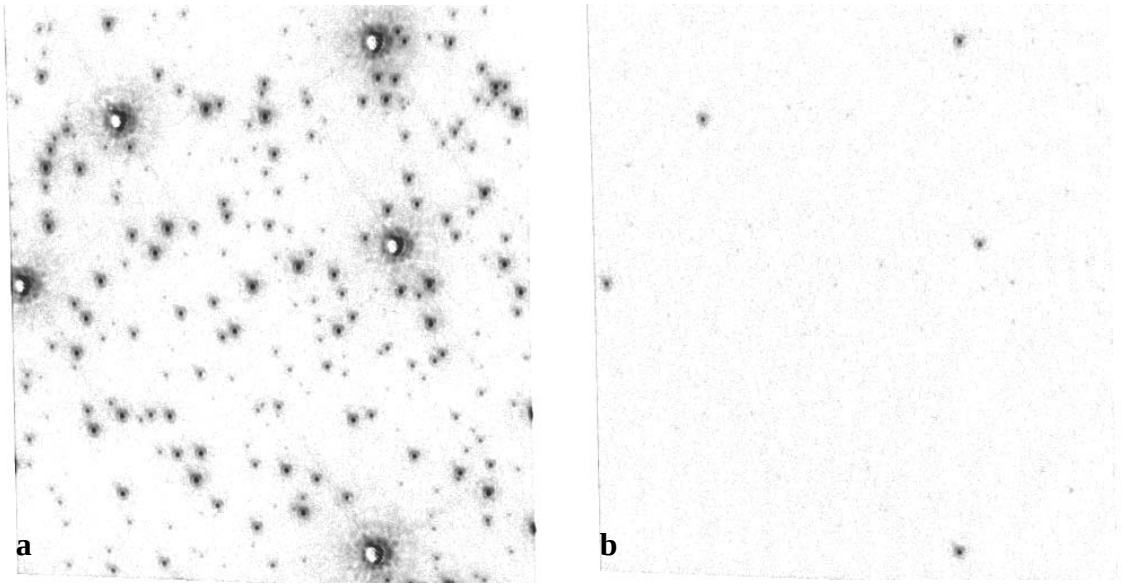

3. Data Analysis

The primary goal of this program was to determine the non-linear behavior of stars in the FOC while also providing the best stellar photometry data for determining the throughputs of the individual ND filters used in the program. The calibration of the ND filters would be a relatively straightforward undertaking if all stars were perfectly exposed throughout the entire ND filter range, but stellar images that are optimally exposed through a thick set of NDs suffer from non-linearity when fewer NDs are in place. Furthermore, stars that look nicely exposed through a modest number of NDs become very noisy in the darkest filter combinations. Accurate photometry of these stellar images therefore required some knowledge of the effects of non-linearity, which can masquerade as an excessive amount of attenuation, if not accounted for properly. In order to decouple non-linearity from ND filter transmission, we began by determining the non-linearity relation, assuming the ND transmissions in the CDBS were correct. This relation was then used as a guide for selecting well-exposed measurements of stars to use in determining the ND throughputs.

All of the measurements described in this report are based on core-aperture photometry of the ω Cen stars inside a radius of 5.5 pixels using a background annulus 6-12 pixels in radius from the center. This technique produces point-source measurements whose linearity characteristics were expected to match the linearity characteristics of flat-field data (P. Greenfield, ISR FOC-074). In exposures taken through the clearest filter combinations, the peak pixels of the brightest stars can be highly saturated. Sometimes the center of the PSF drops to nearly zero counts. Centroids for each star were therefore determined from

unsaturated images, and the photometry was done in all the images using the same centroided position for each star.

Frequently this report will quantify the results of this core-aperture photometry in terms of the count rate in the peak pixel, a number that is not explicitly aperture-sensitive. However, photometry using the peak pixel alone is not very accurate. For example, variations in the centering of the PSF within the peak pixel can produce a scatter in the photometry larger than the effects that are being calibrated. Thus, *the 'peak count rates' reported here are actually based on the core-aperture photometry described above*. These 'peak count rates' equal 0.07742 times the count rate in the 5.5 pixel radius aperture and correspond to the count rate expected in the peak pixel, if it were perfectly centered within the aperture. This kind of 'peak count rate' is obviously much less subject to photon shot noise and saturation than the true count rate in the peak pixel.

The stars used to calibrate the ND filters were manually selected for measurement based on their apparent count rate, their isolation from nearby stars, and the degree to which they were located evenly across the entire image. In the image taken through the most opaque filter combination (F6ND+F1ND), 13 stars were chosen that were not too faint for photometry, with peak count rates of at least 5 times the background count rate. These stars were then run through the *phot* task in the *apphot* package of IRAF which performed the core-aperture photometry described above, yielding a total number of background-subtracted counts for each star. Through the more transparent filter combinations, intrinsically fainter stars became measurable and were added to the list of calibration stars. In all, 30 stars were measured in the F6ND, F4ND+F1ND, F4ND, and F2ND+F1ND images, and 35 stars were measured in the F2ND+F1ND, F2ND, and F1ND images. The total number of counts for each stellar image was then divided by the image's exposure time to produce a count rate.

Figure 2 and Figure 3 illustrate how the count rates of particular stars vary when the FOC views those stars through various ND filter combinations at the F430W bandpass. In each figure, the horizontal axis shows the "peak count rate" (see above) for stars seen through a particular filter combination, and the vertical axis shows the ratio of count rates between this and another less transparent filter combination. The horizontal lines in each figure indicate the count-rate ratios predicted by the pre-flight ND filter calibrations. These lines always appear at ratios below unity because the more transparent filter set always supplies the denominator.

Three trends are evident:

1. At peak count rates greater than 2 counts s^{-1} pix^{-1}, stellar images in the more transparent filters saturate, and the observed throughput ratios rise.
2. At low peak count rates, noise dominates the stellar images taken through both filters, and the throughput ratios approach unity (as seen in Figure 3).

Figure 2: Ratios of ND combinations. Solid line represents the expected ratio as determined using synphot.

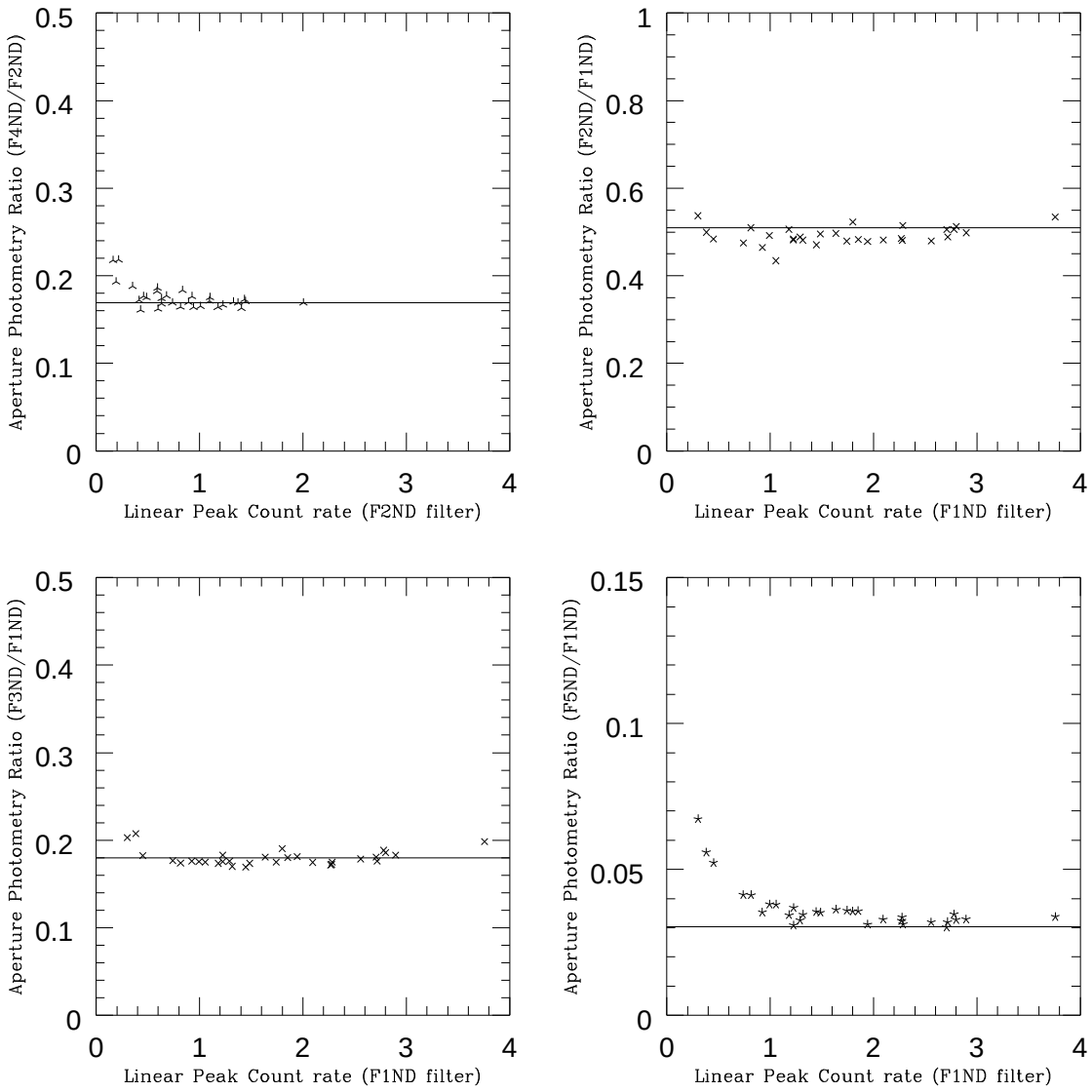

3. In between these regions of systematically deviant behavior, the count-rate ratios lie reasonably close to their predicted values

In order to quantify how closely the observed throughput ratios agree with expectations, level lines were fit to the data in between the realm of saturation and the realm of noise. The realm of saturation was taken to be at peak count rates exceeding 2 counts s^{-1} pix^{-1}, and the realm of noise was taken to be below a total count rate within the aperture of 0.02 counts s^{-1} pix^{-1} through the more opaque filters. The results of these fits, along with the associated errors (1σ), are given in Table 2, and the associated transmissions for each individual filter are given in Table 3. For brevity, we express combinations like F2ND+F1ND as F3ND. Filters F1ND and F2ND appear to agree quite well with the pre-

Figure 3: Ratios of more ND combinations. Solid line represents the expected ratio as determined using synphot.

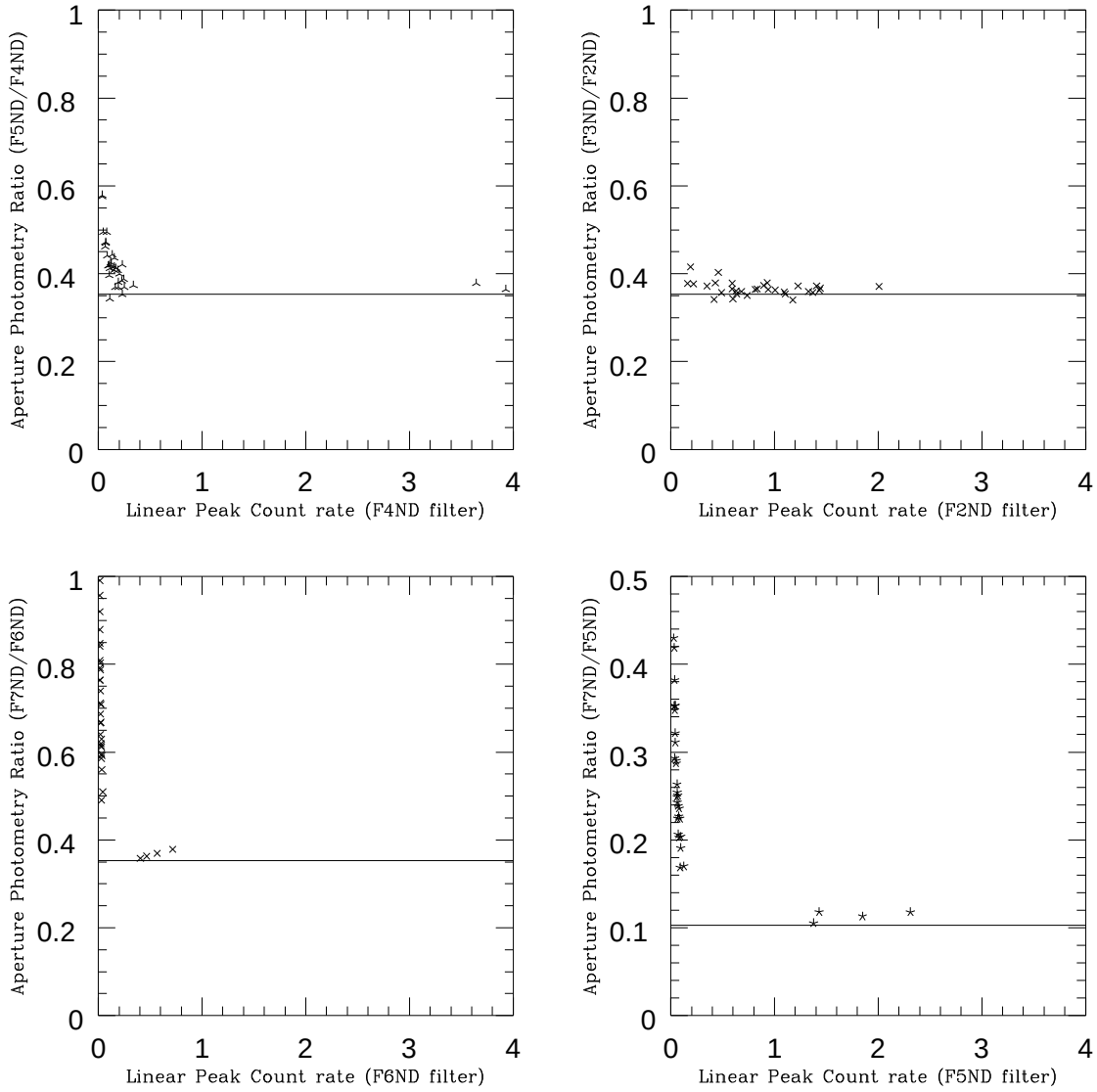

launch calibrations, at least in the F430W region. Filter F4ND could be ~ 10% more transparent than listed in the calibration database, and the filter F6ND throughput agrees with pre-launch calibration within a very large error margin of 30% (1σ).

Table 2. Filter Throughput Ratios in F430W

Filter Ratio	Predicted	Observed	Obs./Pred.
F3ND/F2ND	0.353	0.364 ± 0.013	1.031 ± 0.037
F5ND/F4ND	0.353	0.397 ± 0.027	1.125 ± 0.076
F7ND/F6ND	0.353	0.367 ± 0.009	1.040 ± 0.026
F2ND/F1ND	0.510	0.488 ± 0.021	0.957 ± 0.041
F3ND/F1ND	0.180	0.178 ± 0.005	0.989 ± 0.028
F4ND/F2ND	0.169	0.175 ± 0.014	1.036 ± 0.083
F5ND/F1ND	0.0304	0.0335 ± 0.0019	0.971 ± 0.062
F7ND/F5ND	0.103	0.127 ± 0.029	1.233 ± 0.282

Table 3. Filter Throughputs in F430W

Filter	Method of Calibration	Observed	Obs./Pred.
F1ND	F3ND/F2ND	0.364 ± 0.013	1.031 ± 0.037
(Pred: 0.353)	F5ND/F4ND	0.397 ± 0.027	1.125 ± 0.076
	F7ND/F6ND	0.367 ± 0.009	1.040 ± 0.026
F2ND	F3ND/F1ND	0.178 ± 0.005	0.989 ± 0.028
(Pred: 0.180)	F2ND/F1ND x F5ND/F4ND	0.194 ± 0.016	1.078 ± 0.089
	F2ND/F1ND x F7ND/F6ND	0.179 ± 0.009	0.994 ± 0.050
F4ND	F5ND/F1ND	0.0335 ± 0.0019	1.102 ± 0.063
(Pred: 0.0304)	F4ND/F2ND x F3ND/F1ND	0.0312 ± 0.0026	1.026 ± 0.087
F6ND	F7ND/F5ND x F5ND/F1ND	0.00426 ± 0.0010	1.361 ± 0.320
(Pred: 0.00313)			

Since most of the ND filters are moderately well calibrated, they can be used to construct a non-linearity relation for point sources in the FOC. This exercise provides a check on the assumption that saturation is minimal below 2 counts s^{-1} pix^{-1}. Point-source count

rates through the most opaque filter combinations are the least saturated. For each star the fiducial count rate was taken to be the lowest count rate at which the star was still well-exposed. These fiducial count rates range from 1-2.6 counts s^{-1} in the full aperture, corresponding to peak count rates of 0.05 - 0.16 counts s^{-1} pix^{-1}. Assuming no saturation, expected count rates for the same star seen through more transparent filters were then computed using the pre-launch calibrations to bootstrap upwards to higher throughputs. Figure 4 compares these expectations with the actual "peak count rates" for each stellar image.

Figure 4: Linearity relation for stars based on photometry done in a 5.5 pixel radius aperture compared to the flat-field linearity curve.

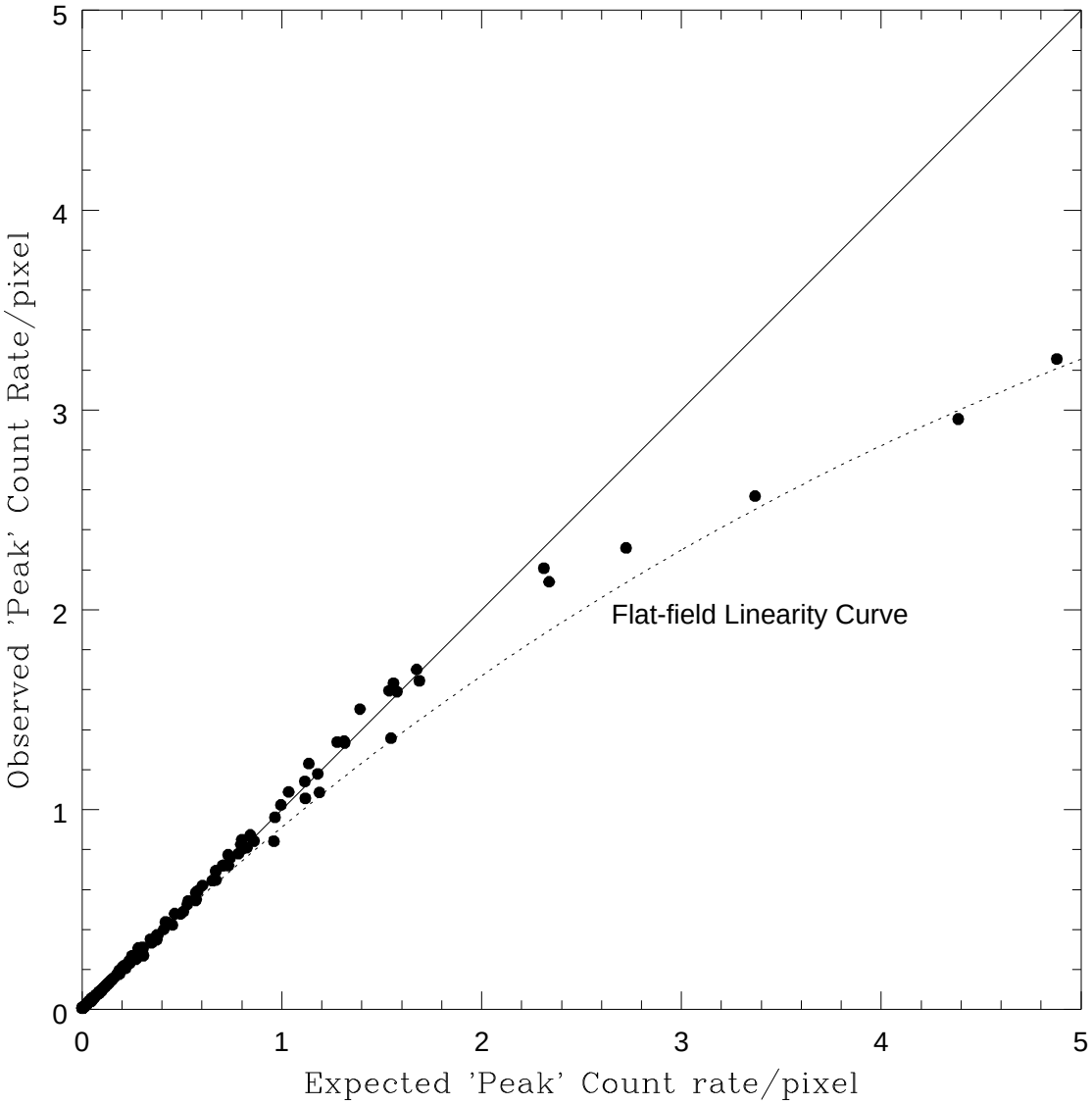

Figure 5: Measured count rates per pixel in the 5.5 pixel apertures compared to the flat-field linearity curve.

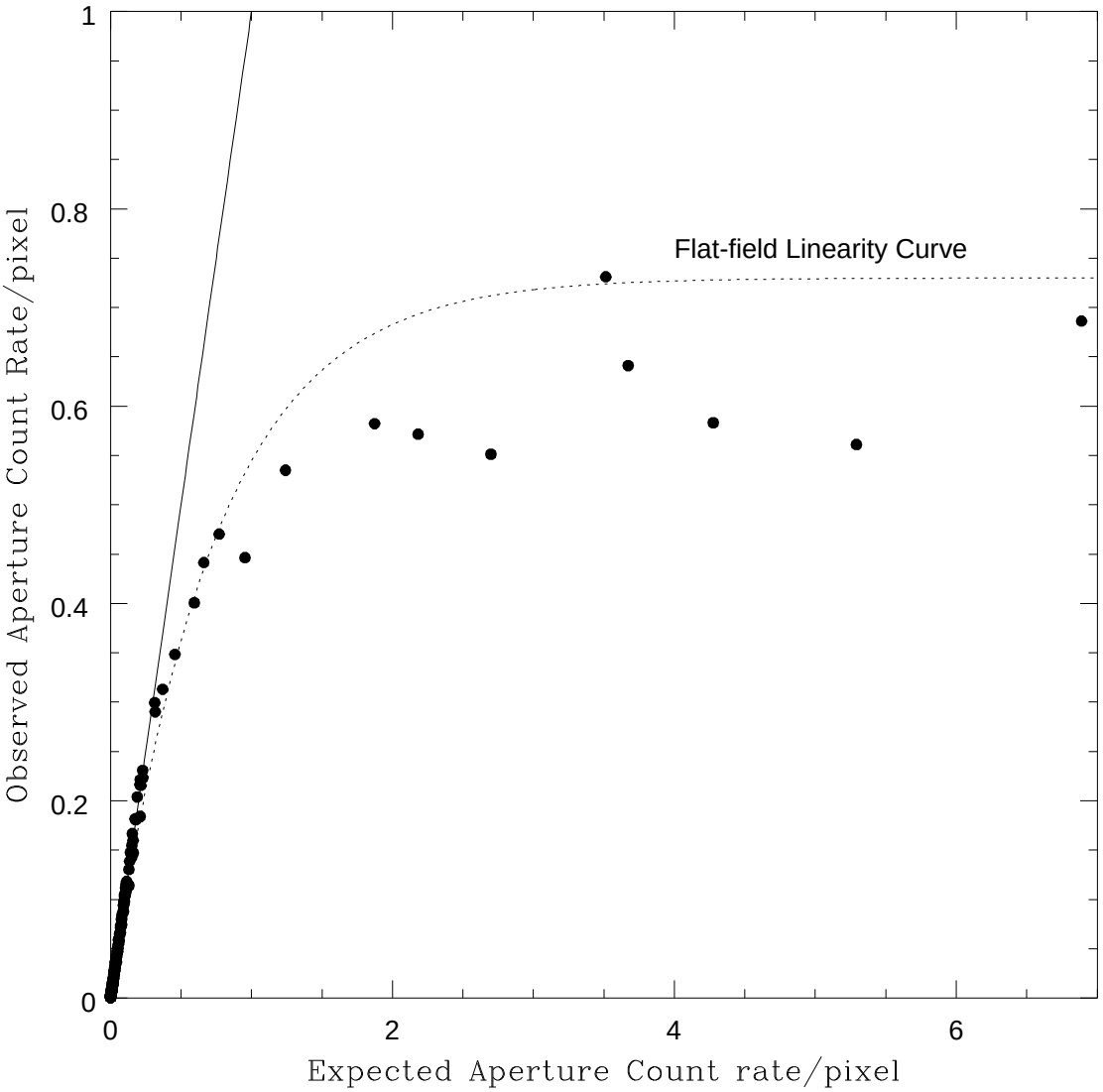

Expectations agree closely with reality up to count rates greater than 2 counts s^{-1} pix^{-1}, at which point expectations no longer keep pace. This peak count rate marks the point where saturation begins to compromise the accuracy of FOC point-source photometry. From there onward the linearity curve flattens out, and the actual "peak count rates" based on photometry with a 5.5 pixel radius never exceed 5 counts s^{-1} pix^{-1}. Below rates of 2 counts s^{-1} pix^{-1}, discrepancies between the pre-launch calibrations and the current ND throughputs can potentially lead to systematic deviations from linearity: a 10% discrepancy would produce a systematic 10% deviation. Even so, the adherence to a linear relation looks remarkably tight, and there is no apparent evidence for saturation in this regime.

Figure 6: Photometry of stars from each image compared to expected peak count rate. Each star is labelled by the ND number of the image which served as the basis for determining the expected count rate.

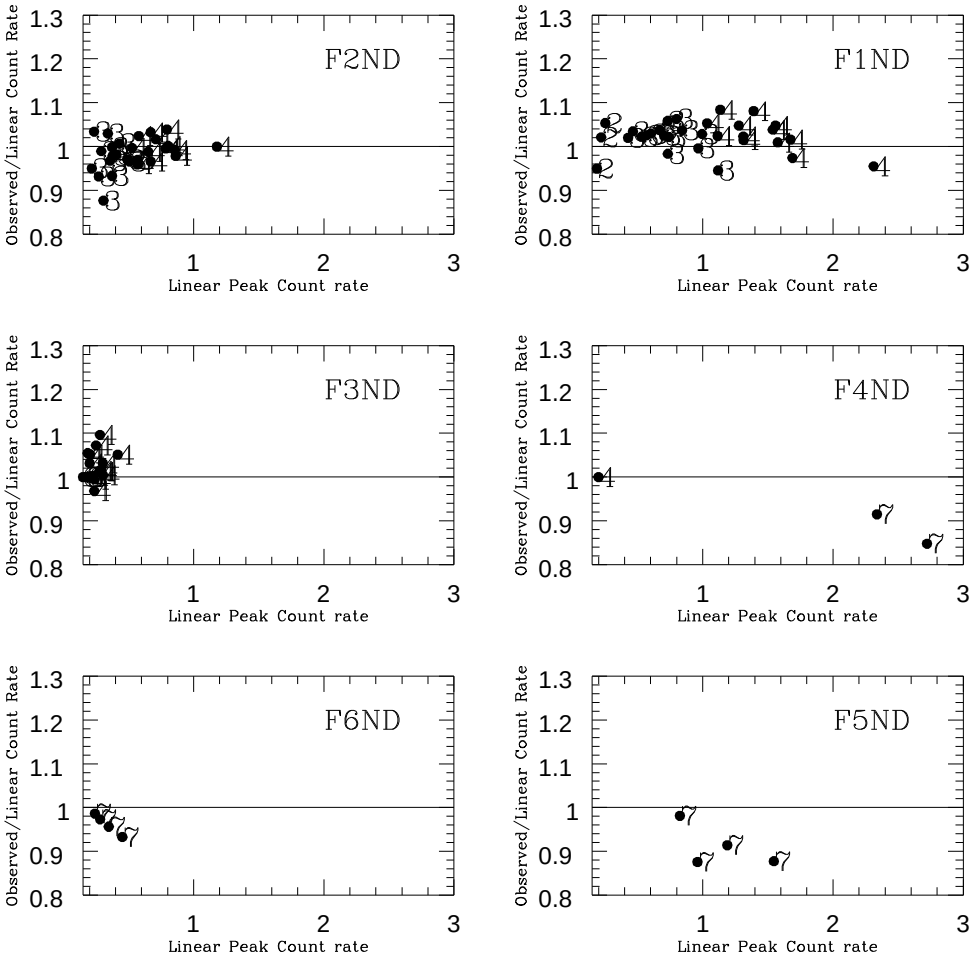

4. Comparisions with Previous Calibration

Alas, the ND filter calibrations given in Table 3 are not easily reconciled with a previous set of in-orbit calibrations done with the blue LED internal to the FOC. Calibration proposal 5525 by P.Greenfield and P. Hodge obtained several f/96 256x256 flat-field exposures through the CLEAR, F1ND, F2ND, and F4ND filters, using the blue diode for illumination. Count rates were measured within five quadrangles defined by four adjacent reseau marks, to minimize the impact of geometric distortion. The intensity of the LED was carefully controlled to keep saturation below 7%, and the count rates were passed through the routine `fflincor` to correct for non-linearity. The resulting count rate per pixel in each of the five quadrangles differed by of order 1% in each case, although the actual count-rate uncertainties are suspected to be somewhat higher. Table 4 and Table 5 give the measured throughput ratios for the flat-field images, along with the throughputs

for individual filters and the corresponding results from Table 3. Note that the predictions for the F430W images and the blue LED images differ somewhat because the ND filters are not perfectly gray and the F430W bandpass is not identical to the blue LED intensity curve (see Figure 7).

Figure 7: Comparison between F430W, F470M, and Blue LED transmissions. The throughputs determined from the F430W observations (X) and the LED images (dot) are plotted at the central wavelength for their respective passband.

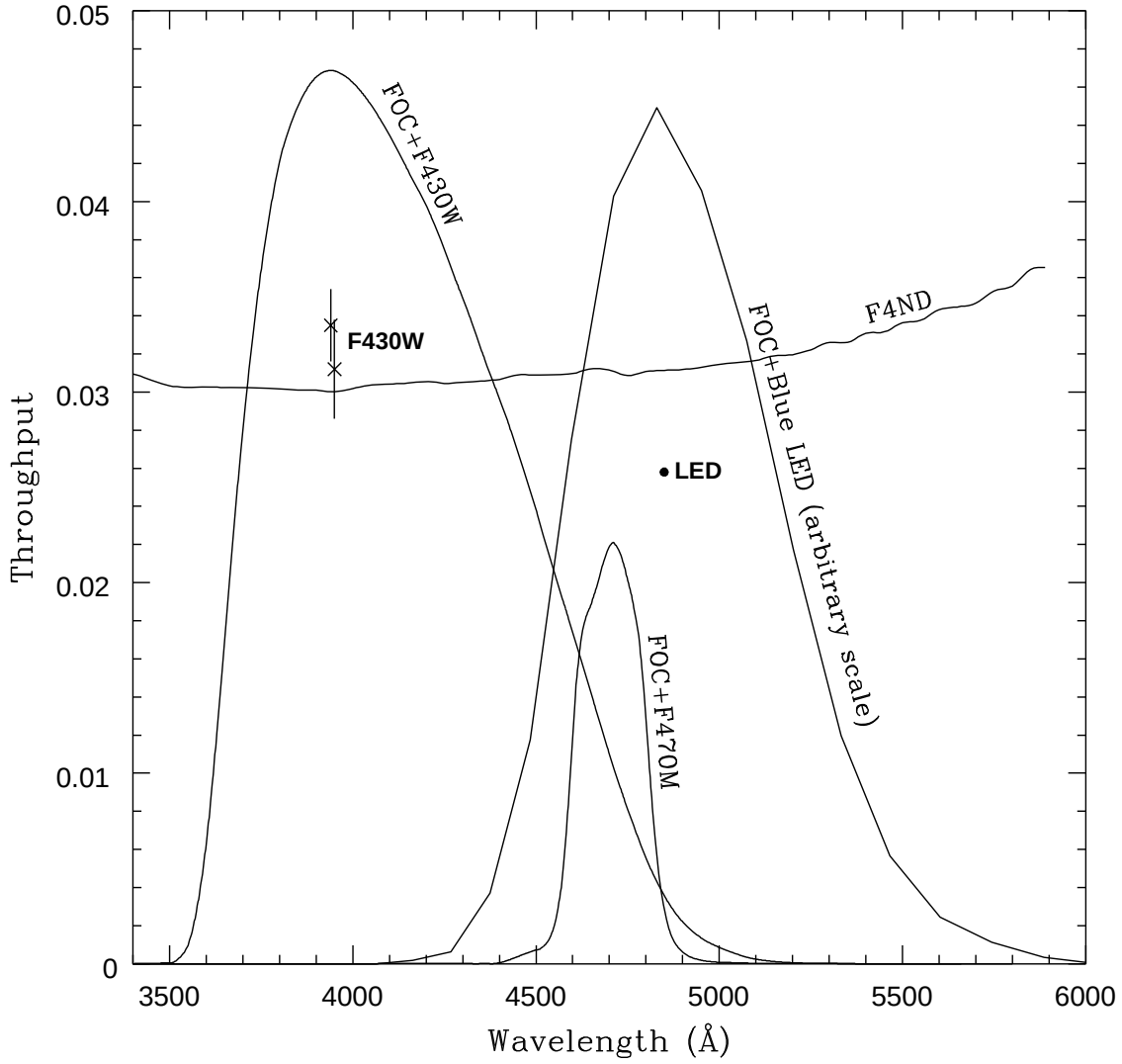

Table 4. Throughput Ratios for the Blue LED (483 nm) Flat Fields

Filter Ratio	Predicted	Observed	Obs./Pred	Obs./Pred. (F430W 2σ range)
F1ND/CLEAR	0.3319	0.3392	1.022	0.988 - 1.092 (F7ND/F6ND)
F2ND/F1ND	0.5036	0.4515	0.897	0.875 - 1.039
F4ND/F2ND	0.1872	0.1685	0.900	0.870 - 1.202

Table 5. ND Filter Throughput Comparison

Filter	LED Obs.	LED Obs./Pred.	F430W Obs./Pred. 3σ range
F1ND	0.3392	1.022	0.962 - 1.118 (F7ND/F6ND)
F2ND	0.1532	0.9164	0.905 - 1.073 (F3ND/F1ND)
F4ND	0.0258	0.8253	0.913 - 1.291 (F5ND/F1ND)

While the discrepancies in the measured ratios are within the 2σ error limits, the trend toward excess opacity in the flat-field measurements of the darker filters leads to a throughput for F4ND that differs from the F430W point source measurements by more than 3σ. The reason for this discrepancy is not yet clear. In order to rule out irregularities in the data handling, we rereduced the flat-field data and obtained the same count rates as before. Another potential contributor to the discrepancy is the difference in the uniformity of the illuminating sources. This, too, appears unlikely to be the culprit. Even though it is more difficult to subtract background counts from a flat field, the expected background count rate of 7×10^{-4} counts s^{-1} pix^{-1} is less than 1% of the total in the flat-field images. Differences in the non-linearity corrections also fail to account for the discrepancy. The correction applied to the raw flat-field data reduces the measured F4ND/F2ND ratio by 6%, so even the uncorrected data deviate significantly from the F430W measurements of ω Cen. The point-source measurements themselves have not been corrected for saturation, but any such correction would be just as small. Saturation manifests itself as an upward slope in the measured throughput ratio plots. However, the measured ratios look quite flat up to 2 counts s^{-1} pix^{-1}. In the F3ND/F2ND vs. F2ND and F3ND/F1ND vs. F1ND plots in particular, the ratios are constant to 4% within the sampled range, indicating that systematic errors owing to saturation must be smaller.

The only explanation of this discrepancy consistent with all the available data is that the difference between the pre-launch calibration of F4ND and the current throughput changes as a function of wavelength. Figure 5 illustrates the kind of deviation that would be required. It compares the F430W and LED results with the transmission curve for the F4ND filter. While the curve for the F4ND filter remains relatively flat across the F430W and Blue LED passbands, the inferred curve between the F430W and Blue LED results (X

and dot respectively) declines by at least 10%. The F4ND throughput apparently remains relatively close to nominal from 3500-4500Å but. drops below nominal in the 4500-5500Å region.

5. Future ND Filter Calibrations

One way to test the wavelength dependence of the ND filter throughputs is to observe crowded star fields through different bandpasses. The F470M filter has a transmission curve quite close to the intensity curve of the blue LED (see Figure 7). Observing ω Cen through this filter, in combination with various ND filters, would help to isolate the effects of wavelength dependence. Such a set of observations has been included in the FOC Cycle 6 calibration program.

The Cycle 6 calibration program will also include similar observations of R136A to measure the UV throughputs of the ND filters. This star cluster will be observed through the F253M filter in tandem with ND filters ranging from F1ND to F6ND. This set of observations will establish the large-scale slope of the ND throughputs from the blue to the UV. In addition, observations of R136A through F1ND, F4ND, and F1ND+F4ND at F190W will be used to test the shorter-scale wavelength dependence of the F4ND filter (and the F1ND filter) in the far-UV.